I. Project Research

Project 3

PR3 Project Research on Development of Scattering Spctrometers Utilizing Small and Medium Class Neutron Source

M. Sugiyama

Research Reactor Institute, Kyoto University

Objectives and Allotted Research Subjects: The aim of this project is to evaluate and improve the possibility of small-angle neutron scattering (SANS) utilizing small and medium class neutron source since KUR-SANS, KUMASANS, is one of typical examples of SANS spectrometers installed at medium class neutron source. However, in this year, there was no enough machine times because of no operation in the first half year and the commissioning in the later half year. Under this circumstance, some works were performed with small-angle x-ray scattering spectrometers in our laboratory, or the others were carried out with SANS spectrometer in other facilities.

ARS-1: Determination of degree of deuteration level of deuterated protein through small-angle neutron scattering. (R. Inoue, K. Morishima, N. Sato, M. Sugiyama)
ARS-2: A saxs study on the nanostructure of gliadin hydrates with sodium chloride. (N. Sato, R. Urade, Y. Higashino, R. Inoue, K. Morishima, M. Sugiyama)
ARS-3: Characterization of Nanostructure in Metallic Materials using Small-Angle Scattering. (Y. Oba, N. Sato, R. Inoue and M. Sugiyama)
ARS-4: Nanostructure of Hydrated α-, γ-, ω-Gliadins. (R. Urade, Y. Higashino, Y. Kitao, N. Sato, M. Sugiyama, R. Inoue and Y. Sakamaki)
ARS-6: Nano structure of metal hydride by X-ray small angle scattering. (K. Iwase, K. Mori, Y. Oba, R. Inoue, M. Sugiyama)
ARS-7: Radius of Gyration of Polymer for Viscosity Index Improver at Various Temperatures Evaluated by Small-Angle X-Ray Scattering. (T. Hirayama, R. Takahashi, K. Tamura, N. Sato, M. Sugiyama, M. Hino, Y. Oba)

Main Results and Contents of This Project:

ARS-1: Inoue et.al. have determined the degree of deuteration level of deuterated protein through SANS method with Quakka in ANSTO. The control of deuteration level of deuterated protein is a key technology in the next genera-tion of neutron biology.

ARS-2: Sato et.al. investigated the nanostruc-ture of gliadin hydrates with sodium chloride us-ing an in-house SAXS instrument (NANO-PIX, Rigaku) installed at Institute for Integrated Ra-diation and Nuclear Science, Kyoto University, instead of SANS. He shows the addition of NaCl makes the contraction effect of NaCl to the glia-din hydrates.

ARS-3: Oba et.al. are challenging that the characterization of nanostructure in metallic materials using both small-angle x-ray scattering and small-angle neutron scattering. In this year, his group mainly used an in-house SAXS instrument with Mo source (NANO-viewer, Rigaku) installed at Institute for Integrated Radiation and Nuclear Science, Kyoto University, and proved that Mo radiation is useful for the metallic materials even with in-house source.

ARS-4: Urade et.al. are investigating wheat flour dough of which physical properties mainly depend upon the wheat protein Gliadin. In this study, her group studied the structural difference of types of Gliadins, α-, γ-, ω-gliadins, in nano scale. SAXS analyses suggested that the C-teminal helix-rich structures of α- and γ-gliadins may cause the density fluctuation inside aggregates.

ARS-6: Iwase et.al. studied nano structure of metal hydride by Mo-source-X-ray small angle scattering (NANO-viewer, Rigaku), which is installed at Institute for Integrated Radiation and Nuclear Science, Kyoto University. The fractal dimension of the particle surface was estimated from the slope of a SAXS profile. As a result, the particle surface of Pr2Co7 was smooth.

ARS-7: Hirayama et.al. evaluated polymer viscosity index improver at various temperatures with small-angle x-ray scattering by an in-house SAXS instrument (NANO-PIX, Rigaku) installed at Institute for Integrated Radiation and Nuclear Science, Kyoto University. The result indicates that Olefin copolymers form largesized aggregate with a fractal-like structure in squalane even when the concentration was low, but the result conflicts from the past perception.

PR3-1 Determination of Degree of Deutteartion Level of Deuterated Protein Through Small-angle Neutron Scattering

R. Inoue, K. Morishima, N. Sato and M. Sugiyama

Research Reactor Institute, Kyoto University

INTRODUCTION: Small-angle Neutron (SANS) technique gives the overwhelming opportunity for structural analyzes on various target samples. Especially, contrast-variation SANS (CV-SANS) technique [1], which utilizes the modulation of scattering contrast between solute and solvent, offers the better opportunity for studying the partial structure of complex biomacromolecules. However, the procedure for determining the degree of deuteration level of prepared deuterated biomacromolecules has not been well established up to now. We then try to utilize SANS technique for the determination of degree of deuteration level of deuterated protein. As a first trial, we prepared partially deuterated protein, which was expected to be contrast matched with D_2O. We try to verify whether or not such prepared partially deuterated protein is experimentally invisible in D_2O by SANS.

EXPERIMENTS: We firstly prepared 75% deuterated αB-crystallin by tuning the mixing ratio of hydrogenated and deutearted glucose in 75% D_2O. Prior to the SANS measurement, we also performed small angle X-ray scattering (SAXS) measurement with 75% deuterated αB-crystallin to check the absence of aggregation. SAXS mesurements were performed with NANOPIX (Rigaku Corporation, Japan) equipped with HyPix-6000. A Cu K-α line (MicroMAX-007HF) was used as a beam source, which was further focused and collimated with a confocal multilayer mirror. Since KUMASANS, which is installed at our institute is still on the way to restart. Hence, SANS measurements on prepared 75% deuterated αB-crystallin was performed with QUOKKA installed at Australian Nuclear Science and Technology Organization (ANSTO). The wavelength of neutron and sample to detector distance was 6 Å and 8 m, respectively. To modulate the scattering contrast, we prepared 75% deuterated αB-crystallin in 0%, 60% and 100% D_2O. All the SAXS and SANS measurements were performed at 37 ^oC.

RESULTS: Fig.1 shows SAXS profile from 75% deuterated αB-crystallin at the concentration of 0.45 mg/mL. It can be clearly seen the absence of upturn at low Q region. From the Guinier analysis, the radius of gyration ($\underline{R}_g$) was estimated to 52.8±1.0 Å and this size is consistent with that reported in our previous results [2]. Fig. 2 (a) shows the concentration scaled SANS profiles from 75% deuterated αB-crystallin in 0%, 60% and 100% D_2O, respectively. With increasing the volume fraction of D_2O, the scattering intensity tends to decrease, implying the decrease of scattering contrast. Fig. 2 (b) indicates the volume fraction of D_2O dependence of $(I(0)/c)^{0.5}$, which is nearly comparable to scattering contrast. In accordance

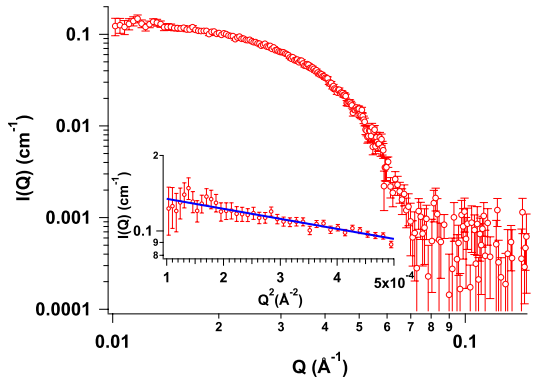

Fig. 1 SAXS profile from 5% deuterated αB-crystallin at the concentration of 0.45 mg/mL. Inset indicates the result of Guinier analysis.

with the tendency shown in Fig. 2 (a), $(I(0)/c)^{0.5}$ decreased with increasing the volume fraction of D_2O. $(I(0)/c)^{0.5}$ intersected with $(I(0)/c)^{0.5}$=0.0 at 97.5 % D_2O, certificating the nearly contrasted with 100% D_2O. As a

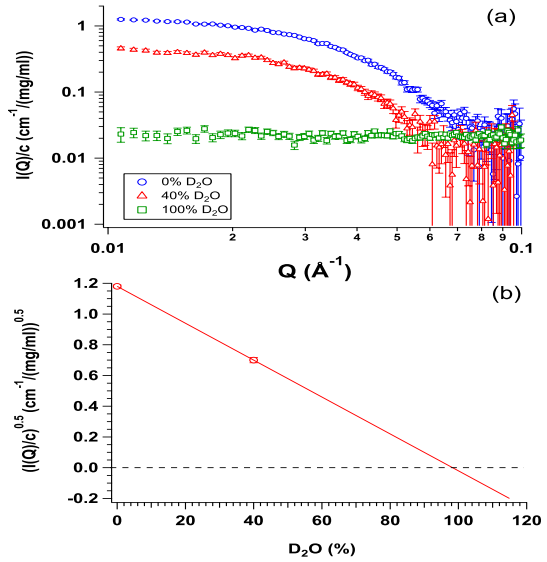

Fig. 2 (a) SANS profile from 75% deuterated αB-crystallin in 0%, 40% and 100% D_2O. (b) The volume fraction of D_2O dependence of $(I(0)/c)^{0.5}$.

next step, we will prepare different deuteration level of deuterated protein and further check the reliability of determination of degree of deuteration of protein with SANS.

REFERENCES:

[1] M. Sugiyama *et al.*, BBA, **1862** (2018) 253-274.
[2] R. Inoue *et al.*, Sci. Rep. **6** (2016) 29208.

PR3-2 A SAXS Study on the Nanostructure of Gliadin Hydrates with Sodium Chloride

N. Sato, R. Urade, Y. Higashino[1], R. Inoue, K. Morishima, and M. Sugiyama

Institute for Integrated Radiation and Nuclear Science, Kyoto University

[1]Graduate School of Agriculture, Kyoto University

INTRODUCTION: Since ancient times a wide variety of wheat flour foods have been produced and consumed worldwide. Wheat flour foods with high quality and processability can be made from wheat dough having proper physical properties. As is well-known, physical properties of wheat dough is mainly ascribable to those of gluten formed in the dough. More in detail, gluten is composed of two major wheat proteins: gliadin and glutenin. Gliadin is responsible for viscous behavior of gluten, while glutenin is for elastic behavior of it. Therefore it is essential to clarify the nature of these proteins for thorough understanding of physical properties of wheat dough. It had been known that gliadins were only soluble in 60–70% ethanol-water solutions or dilute acids. However recent study revealed that gliadins can be extracted into pure water from NaCl-containing dough [1], which enables the investigation of wheat proteins in the environment more similar to real dough. From this point of view, we have been studying the nanostructure of gliadins in aqueous solutions or hydrates by small-angle X-ray scattering (SAXS) [2]. SAXS is useful for the nanostructural analysis on opaque, disordered and condensed materials, and has been widely employed for the study on soft matters such as polymer gel, colloid and rubber. Our previous study elucidated that gliadin hydrates with a concentration of 40wt% shows a broad peak around scattering vector of 0.4 nm^{-1} in its SAXS profile. This peak indicates the presence of density fluctuation within gliadin aggregates of which the correlation length is ca. 15nm. Furthermore, the addition of NaCl greatly affects the density fluctuation of gliadin hydrates. The peak due to fluctuation gradually diminishes and the correlation length becomes smaller with increasing NaCl concentration. Since the physical properties of gliadins, such as water retention and viscoelasticity, is highly dependent on NaCl concentration, there exists close relationship between nanostructures and physical properties of gliadin hydrates in the presence of NaCl. However, it is still unknown what kind of effect acts on the interaction between gliadin molecules and induces the change of nanostructure of the aggregates. In this study, we carried out SAXS measurements for various gliadin hydrates as different concentrations of urea was added to clarify the mechanism of NaCl effect acting on the association of gliadin molecules.

EXPERIMENTS: Gliadins were prepared by the same method as reported before [1]. Samples were put into 1-nm-thick aluminum cells with optical windows made of 7-μm-thick Kapton film. SAXS measurements were performed with an in-house SAXS instrument (NANO-PIX, Rigaku) installed at Institute for Integrated Radiation and Nuclear Science, Kyoto University. The wavelength of X-ray was 1.54 Å and the camera length was 1300 mm. Typical exposure time was 300 sec. All measurements were carried out at 25 °C.

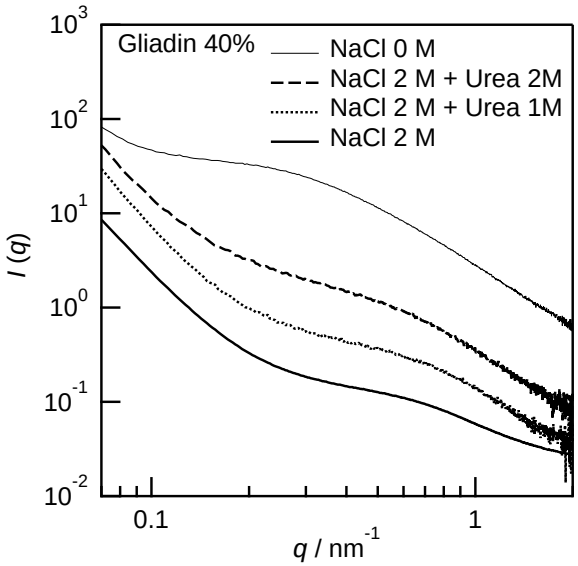

Fig 1. SAXS profiles of 40% gliadin hydrates containing 2 M NaCl together with various concentrations of urea. Each profile is vertically shifted for clarity.

RESULTS: Hydrogen bonding between amino acids of proteins is known to be suppressed in the presence of urea. Therefore, it is expected that influence of hydrogen bonding on the effect of NaCl can be clarified by SAXS measurements for gliadin aggregates with different concentrations of urea. Fig. 1 shows the results. As was same as the previous results, broad peak at q = 0.4 nm^{-1} without NaCl became small and shifted higher to 0.8 nm^{-1} at a NaCl concentration of 2 M. This demonstrates the contraction effect of NaCl to the gliadin hydrates. By adding urea, however, the peak at 0.8 nm^{-1} slightly shifted back to lower q, and the profiles became similar to that of gliadins without NaCl. This suggests that hydrogen bonding between gliadin molecules is partly responsible for the contraction of gliadin hydrates with NaCl. Nevertheless, the change induced by urea was so small that other interaction such as hydrophobic interaction is assumed to be far more dominant to the effect of NaCl on the contraction of gliadin hydrates. Further SAXS experiments to examine intermolecular interaction, for example, measurements of gliadins with deamidation of glutamine residues is now underway.

REFERENCES:

[1] T. Ukai, Y. Matsumura, R. Urade, *J. Agric. Food Chem.*, **56**, (2008) 1122-1130.

[2] N. Sato, et al., *J. Agric. Food Chem.*, **63**, (2015) 8715-8721.

PR3-3 Characterization of Nanostructure in Metallic Materials using Small-Angle Scattering

Y. Oba, N. Sato[1], R. Inoue[1] and M. Sugiyama[1]

Materials sciences Research Center, Japan Atomic Energy Agency
[1]Institute for Integrated Radiation and Nuclear Science, Kyoto University

INTRODUCTION: Small-angle scattering (SAS) is a powerful technique to characterize nanostructures in a wide variety of materials. In particular, SAS is suitable for metallic materials because of the large gauge volume compared to electron microscopy. Another advantage is high penetration power of probe beams (X-ray and neutron). The application of SAS is now spreading into the metallic materials.

However, little opportunity to perform SAS measurements has restricted the further expansion of the SAS application. This is particularly remarkable for small-angle neutron scattering (SANS), which requires large facilities such as research reactors or accelerators.

To overcome this situation, it is necessary to use existing SANS instruments more effective. The SANS instrument CN-2 KUMASANS installed at the Kyoto University research reactor (KUR) plays an important role because it is available for the metallic materials [1]. Further improvement of the CN-2 KUMASANS is effective for the metallic materials.

Another solution is the support by small-angle X-ray scattering (SAXS). It is relatively easy to access to laboratory-scaled SAXS instruments, which can provide plenty of machine time. Structural information obtained by SAXS is basically same as that by SANS. In this study, the improvement of the CN-2 KUMASANS was first carried out for more effective use targeting the metallic materials. In addition, the new SAXS instrument installed at the Integrated Radiation and Nuclear Science was examined.

EXPERIMENTS: The SANS experiment was conducted at the CN-2 KUMASANS [1]. The SAXS experiments were performed using a SAXS instrument equipped with Mo Kα radiation (Nano-viewer, RIGAKU).

RESULTS: For the CN-2 KUMASANS, a vacuum sample chamber was installed at the sample area, which was previously in air separated from upstream and downstream vacuum chambers by vacuum windows (Fig. 1). As the result, background scattering contributions from air and from the vacuum windows are eliminated. This is effective for vacuum resisting samples such as most metallic materials.

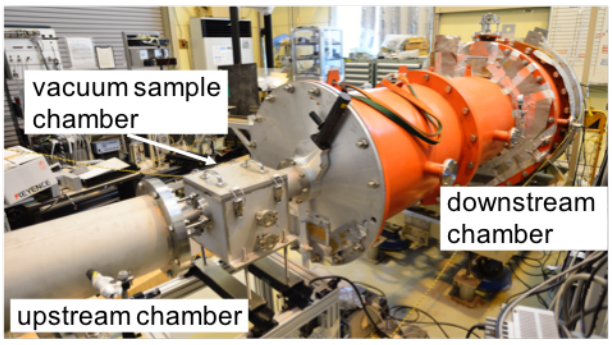

Fig. 1. Vacuum sample chamber installed at the CN-2 KUMASANS.

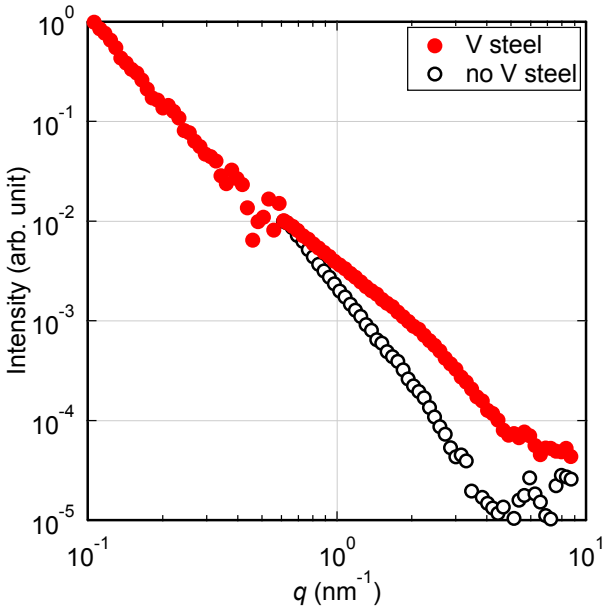

Fig. 2. Typical SAXS profiles of the steels with/without precipitates. Vanadium (V) steel contains the precipitates of vanadium carbide.

Fig. 2 shows the SAXS profiles of the steels containing nanosized precipitates of vanadium carbide. A shoulder around q=2 nm^{-1} is observed. This indicates that the SAXS with the Mo radiation is useful for the metallic materials. Furthermore, a new sample changer was installed in the SAXS instrument. This allows sequential measurements of up to 49 samples. This is important for effective use of the machine time.

REFERENCE:

[1] M. Sugiyama and Y. Maeda, Jpn. J. Appl. Phys., **33** (1994) 6396-6402.

PR3-4 Nanostructure of Hydrated α-, γ-, ω-Gliadins

R. Urade, Y. Higashino, Y. Kitao, N. Sato[1] M. Sugiyama[1], R. Inoue[1] and Y. Sakamaki[1]

Graduate School of Agriculture, Kyoto University
[1] Research Reactor Institute, Kyoto University

INTRODUCTION: Rheological properties of wheat flour dough are dependent on the physical properties of gluten. Gluten consists mainly of two types of proteins: glutenins and gliadins [1]. Among them, gliadins are composed of α-, γ- and ω-gliadins and responsible for the viscosity of dough [2]. Since gliadins are monomeric proteins, gliadin nanostructure formed by noncovalent intermolecular associations are thought to be responsible for its viscoelastic properties. Hence, detailed analysis on nanostructure of gliadins are essential to understand the rheological properties of hydrated gliadins at the molecular level. In this study, we fractionated α-, γ- and ω-gliadins and performed SAXS analysis of the each hydrated α-, γ- and ω-gliadins.

EXPERIMENTS: Gliadins were isolated from wheat flour by the method established previously [3, 4]. Each gliadins was separated by using a column embedded with SP Sephadex C-50 resin (GL Sciences) and eluting with elusion solution (2M urea, 0.04M ethlendiamine, 0.08M HCl pH 3.1). Gliadins in the eluted fractions were determined by western blot analysis after SDS-PAGE. Anti-α-gliadin or γ-gliadin serum for western blot analysis were prepared using recombinant C-terminal domains of α-gliadin or γ-gliadin expressed in *E. coli*. The separated gliadins were subjected on the gel filtration column chromatography on a SPS C-50 column (GL Sciences) equilibrated with 2M Urea, 0.05M NaCl, CH_3COOH pH3.1. once or twice to remove contaminated glutenins. The purified gliadins were dialyzed against distilled water and lyophilized. SR-VUV CD spectra of gliadins were measured at BL12 of the Hiroshima Synchrotron Radiation Center (HiSOR). A nanostructure of gliadins in distilled water was investigated by SAXS analysis. SAXS experiments were carried out with NANOPIX (Rigaku) in Kyoto University Research Institute (KURRI) or at the beam line BL-10C of Photon Factory, a synchrotron radiation facility of Institute of Materials Structure Science, High Energy Accelerator Research Organization (KEK). The dilute solution samples were measured in an aluminum cell with 20-μm thick quartz windows, while viscous hydrated solids concentrated solutions (40 wt%) in a PTFE sandwich cell with windows of 7.5-μm thick Kapton® films (TORAY-DuPont).

RESULTS: Gliadins were separated to three α-gliadin fractions, one γ-gliadin fraction and one ω-gliadin fraction by the first ion-exchange column chromatography. From the SR-VUV CD spectra, contents of α-helix and β-strand of α-, γ- and ω-gliadins were calculated to be 27-31% and 16-19%, 25% and 20%, and 6.2% and 45%.

Guinier and cross-section Guinier analyses of SAXS data from 0.1% gliadins proved that α-, γ- and ω-gliadins in water had a size larger than those in 70% ethanol [5]. At 40 wt%, all gliadins formed gel-like pastes. Alfa-gliadins and γ-gliadins showed SAXS profiles with a shoulder peak at 0.4 nm^{-1} and a steep rise in the low-q region owing to large aggregation. Omega-gliadins showed a SAXS profile with only steep rise in the low-q region. These results suggested that the C-terminal helix-rich structures of α- and γ-gliadins may cause the density fluctuation inside aggregates (Figure 1).

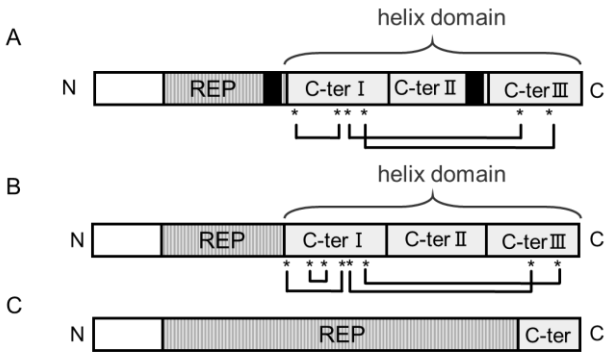

Figure 1 Diagrams representing the structure of gliadins.
A, α–gliadins; B, γ-gliadins; and C, ω-gliadins. The repetitive domains (REP) of α–gliadins, γ–gliadins or ω–gliadins are composed of a single repeat motif of five to eight residues with the following consensus sequence: $P(F/Y)PQ_{3\text{-}5}$, seven to 10 residues with the following consensus sequence: $PFPQQ_{0\text{-}1}(PQQ)_{1\text{-}2}$ or a single repeat motif of six to 11 residues with the following consensus sequence: $PFPQ_{1\text{-}2}PQ_{1\text{-}2}$, respectively. N = N-terminal region, REP = repetitive domain. C-ter I, II, III represent a C-terminal cysteine-rich region, a glutamine-rich region and a terminal conserved sequences. Asterisks represent cysteine residues. All cysteines form in intramolecular disulfide bonds (association lines). α–Gliadins contain two polyglutamine stretches (black bars) in the C-terminal part of the REP domain and C-ter II region.

REFERENCES:

[1] F. MacRitchie and P. L. Weegels. Structure and functional properties of gluten. "Wheat, 4th ed." AACC International Press, 2009.
[2] M. Cornec *et al., J. Cereal Sci.*, **19**, 131-139, 1994.
[3] T. Ukai *et al., J. Agric. Food Chem.* **56**, 1122-1130, 2008.
[4] N. Sato *et al.*, J. Agric. Food Chem. **63**, 8715-8721, 2015.
[5] N. Thomson *et al.*, *Biochim. Biophys. Acta*, **1430**, 359-366, 1999.

PR3-5 Nano Structure of Metal Hydride by X-ray Small Angle Scattering

K. Iwase[1], K. Mori, Y. Oba[2], R. Inoue and M. Sugiyama

Research Reactor Institute, Kyoto University

[1]Department of Materials Science and Engineering, Ibaraki University

[2] Japan Atomic Energy Agency

INTRODUCTION: The phase diagram for a Pr–Co system was previously reported [1,2]. This phase diagram shows nine phases in the equilibrium state: Pr_3Co, Pr_7Co_3, $Pr_2Co_{1.7}$, $PrCo_2$, $PrCo_3$, Pr_2Co_7, Pr_5Co_{19}, $PrCo_5$, and Pr_2Co_{17}. It is known that Pr-Co binary alloys absorb hydrogen. Kuijpers investigated the hydrogen absorption−desorption property of $PrCo_5$. The maximum hydrogen capacity was approximately 0.6 H/M at 294 K. A plateau region was observed in the P-C isotherm. The pressure corresponding to this plateau was 0.05 MPa. The enthalpy of the hydride formation was determined to be -38.5 kJ/mol H_2 from the Van't Hoff plot. The $PrCo_5$-H system was reported by Ichinose et al. and Yamamoto et al. Hydride phases, $PrCo_5H_{2.7}$ and $PrCo_5H_{4.69}$, were prepared by exposing the alloy to hydrogen gas at 1–5 MPa at room temperature. Burnasheva et al. reported on the structure of the hydride phase based on RCo_3 compounds (R = Ce, Pr, Nd, Y, etc.). The maximum hydrogen capacity of $PrCo_3$ reached 1.2 H/M. $PrCo_3$, Pr_2Co_7, and Pr_5Co_{19} all have superlattice structures. The crystal structure of the $PrCo_3$ was previously reported. The alloy was prepared by arc-melting and high-energy milling. After heat treatment, a $PuNi_3$-type structure was obtained. Khan investigated the crystal structure of Pr_5Co_{19} with a Ce_5Co_{19}-type structure. However, the structural information parameter of Sm_5Co_{19}-type Pr_5Co_{19} was not reported.

The present study focused on the nano structural changes that occur during the hydrogen absorption–desorption process of the Pr_2Co_7 with a Ce_2Ni_7-type structure. We paid close attention to the different hydrogenation behaviors of Pr_2Co_7, Pr_2Ni_7, and La_2Ni_7. Detailed nano structural information for $Pr_2Co_7H_x$ was not reported.

EXPERIMENTS: SAXS data were collected using a Rigaku NANO-Viewer with Mo-Kα radiation monochromatized using a confocal mirror and a two-dimensional detector (PILATUS-100k). The voltage and current of the X-ray generator in this measurement were 50kV and 24 mA. The sample was set under vacuum. The incident x-ray was focused using a two-dimensional confocal mirror and collimated using the pinhole technique. The distance between the samples and the detector was 1.06 m, which covers q range from 0.06 to 10 nm-1. The fractal dimension of the particle surface, DS, can be extracted from the slope of a SAXS profile, I(q), in the Porod region, that is,

$I/(q) \propto q^{\alpha}$ (1)

$Ds = 6+\alpha$ (2)

where q is the magnitude of a scattering vector (= $4\pi\sin\theta$ / λ, where 2θ is the scattering angle and λ is the X-ray wavelength). It is a smooth surface as DS is close to 2, but a rough surface as DS is close to 3.

RESULTS: The SAXS profiles of Pr_2Co_7 and $Pr_2Co_7H_{7.2}$ are shown in Fig. 1. Super-reflection peak of Pr_2Co_7 with Ce_2Ni_7-type, 002, and that of the $Pr_2Co_7H_{7.2}$ with orthorhombic, 002, were clearly observed in the q region between 4.10 nm^{-1} and 6.0 nm^{-1}. The shoulder existed in the q region between 1.30 nm^{-1} and 3.90 nm^{-1}, which was caused by $CaCu_5$-type phase. The original alloy consisted of 91% Ce_2Ni_7-type and 9% $CaCu_5$-type. The DS value was obtained from the least-squares fit in the q range between 0.10 nm^{-1} and 0.68 nm^{-1}. As a result, DS was estimated at 1.5 and 2.0, meaning that the particle surface of undeuterated Pr_2Co_7 was smooth.

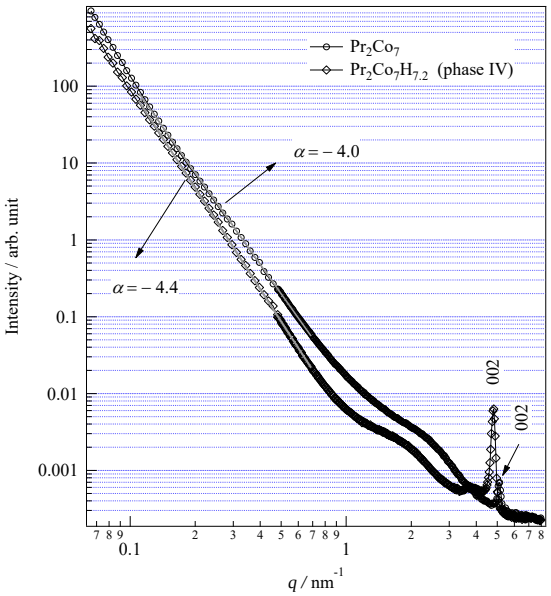

Fig. 1 SANS profiles, $I(q)$, for Pr_2Co_7 and $Pr_2Co_7H_{7.2}$ (H/M = 0.8)

REFERENCES:

[1] Ray AE., A review of the binary rare earth-cobalt alloy systems. Coblat 1974;1:13-8.

[2] Okamoto H. editor. Binary alloy phase diagrams. 2nd ed. Ohio: ASM International, Materials Park; 1996. plus updates.

PR3-6 Radius of Gyration of Polymer for Viscosity Index Improver at Various Temperatures Evaluated by Small-Angle X-Ray Scattering

T. Hirayama, R. Takahashi[1], K. Tamura[2], N. Sato[3], M. Sugiyama[3], M. Hino[3]and Y. Oba[4]

Dept. of Mechanical Eng., Doshisha University
[1]Dept. of Mechanical Eng., Graduate School of Doshisha University
[2] Idemitsu Kosan Co., Ltd.
[3]Institute for Integrated Radiation and Nuclear Science, Kyoto University
[4]Japan Atomic Energy Agency

INTRODUCTION: Lubricating oils are necessary for friction reduction and high wear durability of sliding surfaces in machine components, and the development of the best oils is strongly required from industry. Viscosity index improver (VII) is a kind of additives for relieving the reduction of viscosity of lubricating oil due to temperature rise. Classical textbooks say that the VII molecules work with changing their equivalent radius in base oil in accordance with oil temperature. However, there are only few papers investigating the equivalent radius of VII molecules by small-angle X-ray scattering (SAXS) and/or small-angle neutron scattering (SANS), and there is still room for discussion of the behavior and working mechanism of VII molecules in oil. This study tried to investigate the radius of gyration of several kinds of VII polymers in base oil at various temperatures by SAXS, and the behavior of polymers was checked and discussed.

EXPERIMENT: To investigate the radius of gyration of VII polymer, we used a SAXS instrument (NANOPIX, Rigaku) with a Cu-target X-ray source emitting X-ray with a wavelength of 1.54 Å, a characteristic line of Cu-Kα. The 1.2 mm-thick aluminum cells having a optical windows made of 20-μm thermally-resistant engineering plastic film (Superio-UT, Mitsubishi chemical) was used for the measurement. The cell temperature increased to be 25, 40, 60, 80 and 100ºC in turn, and the last measurement was carried out at 25ºC again after cooling for checking if the VII molecule degenerated or not by heat. Olefin copolymers (OCP) type VII was prepared as a typical one used in engine oil as a first trial. Squalane was used as a model base oil, and the concentrations of OCP into squalane were 0.17, 0.5 and 1.0 mass%.

RESULTS AND DISCUSSION: The SAXS intensity profiles versus scattering vector q from squalane with 0.5 mass%-OCP VII at various temperatures were shown in Fig. 1. The profiles were obtained by subtracting the intensity profiles from pure squalane at each temperature previously measured with the same liquid cell. We can see that the intensity profiles had little change even if the temperature changed. It means that the size and shape of OCP molecules was hardly changed in the observed range regardless of temperature rise, and this result contradicts the fact that the OCP effectively work as VII. The profiles from the squalane with OCP with various concentrations are shown in Fig. 2. Though scattering intensity increased in accordance with the increase in concentration as expected, the slopes of each profile around q=0.1 nm^{-1} were almost same, about $\propto -q^{2.8}$. It indicates that OCP molecules form large-sized aggregate with a fractal-like structure in squalane even when the concentration was low, but the result conflicts from the past perception. We will continue to measure the other types of VII polymers by SAXS to clarify how we should explain the SAXS profiles from oil-soluble polymers in oil.

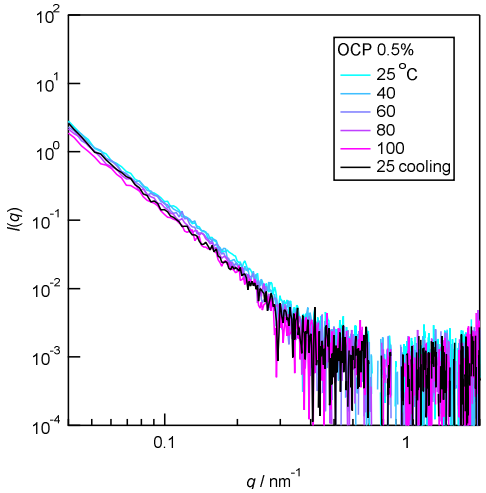

Fig. 1. SAXS intensity profiles from squalane with 0.5 mass%-OCP VII at various temperature.

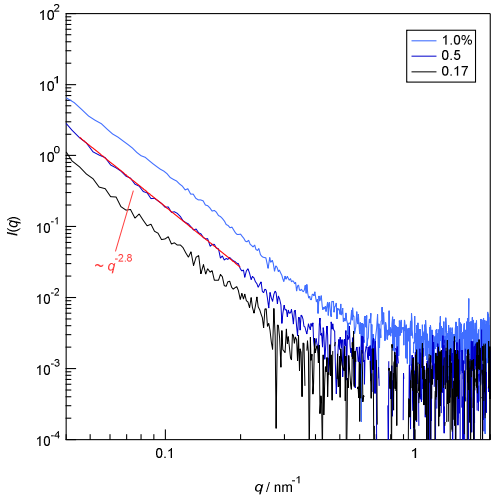

Fig. 2. SAXS intensity profiles from squalane with OCP VII with various concentration at 25ºC.